submitte to ID#: BJOPHTHALMOL/2005/089110

Subretinal electrode implantation in the P23H rat for chronic stimulations

J. Salzmann [a], O.P. Linderholm [b], J-L. Guyomard [c,d], M. Simonutti [c,d], M. Paques [c,d,e], M. Lecchi [f], J. Sommerhalder [a], M. Pelizzone [g], D. Bertrand [f], J. Sahel [c,d,e], P. Renaud [b], A.B. Safran [a], S. Picaud [c,d,e]

[a] Service d'ophtalmologie, Hôpitaux universitaires de Genève,1205 Geneva, Switzerland

[b] Microsystems Unit, Ecole Polytechnique Fédérale, Lausanne, Switzerland

[c] INSERM U-592, , Laboratoire de physiopathologie cellulaire et moléculaire de la rétine, Paris, France

[d] Université Pierre et marie Curie Paris-6, Paris, France

[e] Fondation Ophtalmologique A. de Rothschild, Paris, France

[f] Département de neurosciences, Centre médico-universitaire, Geneva, Switzerland

[g] Centre romand d'implants cochléaires, Hôpitaux universitaires de Genève, Geneva, Switzerland

Running title : A subretinal implant in a dystrophic rat

CORRESPONDING AUTHOR: Dr Serge Picaud, Laboratoire de physiopathologie cellulaire et moléculaire de la rétine, INSERM U-592, Bâtiment Kourilsky, 184 rue du Faubourg St Antoine, 75571 Paris Cedex 12
Email: serge.picaud @ st-antoine.inserm.fr
Fax: 003314 9 28 46 05

KEYWORDS: Photoreceptor degeneration, retina, prosthesis, impedance, rat

ABSTRACT

Background: In age-related macular degeneration and inherited dystrophies, preservation of retinal ganglion cells has been demonstrated. This finding has led to the development of various models of sub- or epi- retinal implant in order to restore vision. The present study addresses the development of a polyimide subretinal electrode platform in the dystrophic P23H rat in vivo.

Material and methods: We developed a technique for implanting a subretinal electrode into the subretinal space and stabilising the distal extremity of the cabling on the rat cranium in order to allow future electrical stimulations of the retina.

Results: In vivo imaging of the retina with the scanning laser ophthalmoscope (SLO) demonstrated reasorbption of the surgically induced retinal detachment and the absence of major tissue reactions. These in vivo observations were confirmed by retinal histology. The extraocular fixation system on the rat cranium was effective in stabilising the distal connector for in vivo stimulation.

Conclusion: This study demonstrates that a retinal implant can be introduced into the subretinal space of a dystrophic rat with a stable external connection for repeatable electrical measurements and stimulation. This in vivo model should therefore allow us to evaluate the safety and efficacy of electrical stimulations on dystrophic retina.

INTRODUCTION

In retinal dystrophies and age-related macular degeneration (AMD), visual loss occurs as a consequence of photoreceptor degeneration. As a result, a secondary process of partial trans-synaptic degeneration occurs affecting neurons distal to the degenerating photoreceptors. There is histological evidence of some degree of ganglion cell sparing. [1] [2] [3] [4] [5] Humayun and co-workers have reported that in vivo electrical stimulation of surviving retinal ganglion cells was able to generate phosphenes correlated spatially and temporally with the stimuli, demonstrating that these neurons were still able to convey visual information to the brain. [6] [7] These findings support the assumption that electrical stimulation of surviving retinal cells by a retinal prosthesis might restore useful vision in ARMD or retinal dystrophy. Strategies which have been proposed in order to trigger coordinated ganglion cell activity include subretinal stimulation, [8][9][10] epiretinal stimulation on the retinal inner limiting membrane [11] [12][13][14][15][16] or perineural stimulation around the optic nerve.[17][18]

The efficacy and safety of retinal implants have been investigated in different animal species in vivo. A number of critical issues remain outstanding, such as surgical techniques, stimulation protocols, implant tolerance and biocompatibility.

Subretinal prostheses have been implanted in living wild type pigs and cats where photoreceptors facing the implants eventually underwent degeneration associated with glial tissue formation.[19] The retinal response to light was not however significantly altered by the presence of the implant as indicated by ERG recordings. Retinal stimulation by the subretinal implant also elicited visual-evoked potentials consistent with an activation of retinal ganglion cells.[20][21][22] Self-powered retinal implants have been introduced into the subretinal space of RCS rats,

an animal model of retinitis pigmentosa, in order to demonstrate that the subretinal implant could slow the congenital retinal degeneration.[23] This photoreceptor rescue was ascribed to a trophic effect of the implant on the retina. A similar effect was seen in human experiments where visual performance improved at sites distant from the implant itself.[24]

The aim of this study was to design a surgical approach in vivo in the rat eye using a subretinal implant activated by an external connector in order to evaluate the efficacy and safety of the stimuli on the retina. The dystrophic P23H rat was selected for these experiments because this animal model of retinitis pigmentosa may provide a similar biological environment to patients with inherited photoreceptor degeneration. The study shows that subretinal implants can be inserted for long term-studies.

MATERIALS AND METHODS

Implants

Initial experiments were conducted with inert polyimide (type PI2611) prototypes in order to test the technique and feasibility of the procedure. In later experiments, we implanted devices with one or several platinum electrodes with a 25μm radius. These were produced at the Laboratory of Microsystems, EPFL, using a standard procedure. [25] In brief, a layer of 11 μm polyimide (PI12611, HD Microsystems) was applied by spin-coating, and subsequently cured. A 200 nm-thick layer of platinum was deposited on the polyimide, using titanium as the adhesion layer. The electrodes were shaped using dry etching. A second layer of polyimide was then deposited, and the implant shape and electrode openings were engineered by dry etching. The final total implant thickness was 22 μm. The electrodes were then

soaked in 10% HCl and calibrated using Cole-Palmer® traceable test solutions. To allow diffusion of nutrients and waste products, some implants were also supplied with through-holes with a diameter of 25 µm (Fig 1, 2a).

Animals

Animal experiments were conducted in accordance with the European Communities Council Directive (86/609/EEC) and the Association for Research in Vision and Ophthalmology (ARVO Statement on the Use of Animals in Ophthalmic and Vision Research). Animals were maintained on a normal diet under a 12h light/dark cycle. In all cases, surgery was performed in animals of at least 3 months. After pupil dilatation with a drop of tropicamide (2mg/0.4 ml, Ciba Vision Ophthalmics, Blagnac , France), P23H transgenic rats (line 1) were anaesthetized by intramuscular injection with a 4:1 mixture of ketamine-xylazine (ketamine 100mg/kg, xylazine 10 mg/kg) (Ketamine 500: Virbac, Carros, France; xylazine 2%: Rompun®, Bayer Pharma, Puteaux, France). One eye of each animal was implanted.

Implantation techniques

Once the animal was anesthetized, topical oxybuprocain chlorhydrate 1.6 mg/0.4 ml (Novartis Pharma, 92500 Rueil-Malmaison, France) was instilled on the operated side. A superior conjunctival peritomy was performed. A small radial sclerotomy was made 1.5 mm behind the limbus with a 25G needle. Biolon® (1% sodium hyaluronate, Bio-Technology General, Rehovot, Israel) was injected into the subretinal space through the sclerotomy in order to obtain a localized retinal detachment visible as a clear ‘flush-wave’ posterior to the injection. The polyimide implant was gently inserted anterior to posterior into the subretinal space. The

implant ‘tail’ was sewn to the sclera with 10-0 Nylon. Visual control was obtained with indirect ophthalmoscopy.

In vivo imaging

Scanning laser ophthalmoscope (SLO) images were obtained in 4 rats (Heidelberg Engineering, Heidelberg, Germany). Fluorescein angiograms were obtained by intraperitoneal injection of fluorescein (0.3ml of 4% fluorescein sodium, Fluka Chemie, Buchs, Switzerland). Imaging was obtained without anesthetizing the animals.

Impedance spectroscopy

Impedance spectra were measured with an LCR meter (Agilent 4284A, Palo Alto, USA) controlled by a proprietary Java-software. Measurements were taken between one stimulating electrode and the reference circular electrode. Each spectrum consisted of 60 points logarithmically spaced between 100Hz and 1MHz, with the sweep starting at the highest frequency.

Histology

At 9 weeks animals were anesthetized as described above to allow an intra-cardiac perfusion of 4% paraformaldehyde in phosphate buffer 0.1M (pH= 7.4) at a 10ml/min rate after clamping blood vessels irrigating the inferior part of the body. Once the eye was enucleated, the cornea and lens were removed by circumferential incision anterior to the ora serrata. The implant tail was sectioned in order to maintain the implant head in the subretinal space. Eye cups were incubated overnight at 4°C in phosphate buffer (0,1M ; pH=7,4) containing 4% paraformaldehyde and 2.5%

glutaraldehyde. After several washes in phosphate buffer, the tissue was postfixed in osmium tetroxide 1% for 30 min at room temperature and rapidly rinsed in water. Finally, the tissue was dehydrated in alcohol and embedded in epoxy resin. Semithin sections were obtained by ultramicrotome sectioning (Ultracut®, Leica) with a histo-diamond (45°, 8 mm diatome), and stained with toluidine blue.

RESULTS

Implantation and imaging

Figure 2 shows two different subretinal implants observed in vivo in the fundus. The first implant prototypes were polyimide (type PI2611) bases only to assess the feasibility of the surgical procedure using various head shapes. Implant head diameters > 1mm required large circumferential sclerotomies. Larger prototypes were difficult to adapt to the tight curvature of the eye. Prototypes with a smaller head diameter were also used but were abandoned as they did not provide sufficient space for multiple channel electrodes. Symmetrical head designs were easier to insert under the retina and did not undergo lateral slippage during insertion as was the case for asymmetrical designs. The most suitable prototype had a symmetrical head design with a 1000 µm diameter size and a connecting tail 250 µm large and 4 cm long (fig 2b). These prototypes were 22µm thick.

During this process, 26 rats underwent subretinal implantation in 5 operating sessions. Postoperative examinations confirmed that the implants were in the subretinal space when retinal vessels were seen passing over the device. Fourteen of 26 implants were satisfactorily positioned in the subretinal space (54%); the success rate in the last 10 operated animals was 70%. A number of post-implantation extrusions reduced the very high initial success rate for subretinal space positioning.

After up to 1.5 months, SLO imaging of the retinae showed no fibrous reaction in the vicinity of the implant and macroscopically normal tissue (Fig 2). In one case, however, a hemorrhagic retinal detachment was observed at the level of the implant head.

After establishing the most appropriate shape for the implant we then investigated how an external connector at the distal end of the implant could be made reliably accessible for repeated stimulations and recordings on the living animal. This external connector (6 male pins) connected to the implant tail was glued onto a plexiglass plate with araldite. Implantation was performed under general anesthesia. A cutaneous incision on the cranial apex was performed and 2 small bore-screws inserted into the cranial apex as previously described for the stabilisation of intracerebral injection cannulae. [26] A subcutaneous track was made between the lateral superior fornix of the implanted eye and the skin incision with a 16 G cannula. The implant head was 'fed' through this track distal to proximal before being inserted under the retina. Once the intraocular procedure was completed, the proximal electrical connector plate was fixed with dental cement to the bore-screws in the skull

The rapid curing of the paste provided a stable resting platform for the connector. In order to safeguard it from post-surgical damage, the connector was protected in a casing made out of the proximal end of a screw-top Eppendorf tube. To assess whether stimulations can be applied on non-anesthetized rats, sequential impedance measurements were achieved one week after implantation by applying a 50 mV sine wave at different frequencies. In figure 3A, wires are seen leaving the implant connector on the non-anesthetized rat head and linking up with an LCR meter (seen in the background) via four BNC cables. Figure 3B illustrates the stability of the impedance measurements at 0, 15 and 60 minutes.

Retinal semi-thin sections confirmed that the retinal tissue was not greatly altered in the vicinity of the implant (Fig 4). In average, ganglion cells were observed at a distance of 149.9 µm (± 25.7 µm s.e.m., n=5) from the implant below the retina.

CONCLUSION

This study demonstrated that it was possible to implant platinum electrodes into the subretinal space of the P23H rat and to maintain a stable electrical connection between the electrodes and the extraocular connector, notwithstanding mechanical stress on the connector cable. The implants remained in the subretinal space for up to 1.5 months without histological evidence of glial scarring. The few cases of proliferative vitreoretinopathy were attributed to the surgeon's learning curve.

Subretinal implantation of various implant designs in mammals such as the cat, the rabbit , the non-dystrophic laboratory swine and the RCS rat have previously been reported [24][27]. In the latter, the subretinal implant was self-powered and no external cabling was required [24]. Implantation in the rat, pig and cat has been obtained by elevating the retina with a subretinal fluid injection through a sclerotomy to create an iatrogenic retinal detachment [21][22] [24] [27] [28]. The implantation method is simple and reproducible. Subretinal access is achieved by sclerotomy or sclerectomy without entering the vitreous cavity (ab externo) or by retinotomy or limbal sclerotomy using a vitrectomy approach (ab interno). The latter techniques have been used in rabbits [9], minipigs [29] and cats [30]. Given the size of the rat globe and lens, this approach is not possible with current instrumentation. Zrenner and co-workers developed a custom-made implantation tool for multiphotodiode array (MPDA) implantation in the rat subretinal space [31]. However, these MPDAs were stand-alone devices without the extraocular wire

connexion used in our experiments. Subretinal implants have also been introduced in dystrophic RCS rats in order to demonstrate the neuroprotective effects of implantation, which were noted with both active and inactive implants [24]. These trophic effects, akin to those reported after phosphate buffer injection into the subretinal space [32] were ascribed to the effect of the surgery itself on the retina.

RCS rats have defective phagocytosis of photoreceptor outer segments by the RPE. This results from a recessively transmitted Mertk mutation which is solely expressed in the RPE.[33] In this study we used P23H transgenic rats with the opsin mutation responsible for the most common form of autosomal dominant retinitis pigmentosa (adRP). Line 1 rats, which were used in these experiments, have the highest level of transgene expression and the fastest rate of photoreceptor degeneration. Histopathological and electrophysiological studies have shown broad similarities between human adRP P23H mutation and P23H rat retinal degeneration. [34]

The difference in activation threshold between normal and dystrophic human retina that was reported with epiretinal implants further supports the use of a dystrophic mammal model to evaluate stimulating electrodes and protocols. Although surgery in the rat is difficult given the small globe and large lens [35], dystrophic rats, with a life-span of up to 2 yrs, provide a unique model in which long term stimulation of the retina can be performed. Electrophysiological measurements were recently achieved in vivo on rats just after implantation but were not performed following chronic stimulations. [36] In further studies on P23H rats, which are readily available at a low cost relative to cats or pigs, we plan to investigate the safety and efficacy of long term retinal stimulation using the electrical connector attached to the animal's head as shown in fig 2 as well as changes in electrical impedance over time using

electrical impedance spectroscopy, a technique with which it is possible to simultaneously characterize the conductivity of a tissue sample and the surface properties of the electrodes.[37] The distance between implant and the retinal tissue as observed on histological sections already suggest that appropriate electrical stimulations of retinal cells should produce activation of visual centers.

Various electrode sizes have been implanted into the subretinal space: 8 platinum electrodes of 100 µm x 100µm for direct electrical stimulation of the retina in the pig and rabbit [27], an array of up to 5000 photodiodes with 20µm x 20 µm electrodes powered by incident light in the cat [28], a 2 mm diameter, 25µ thick chip with approximately 5000 independent microphotodiodes in human volunteers [23]

Our prototype has similar sized electrodes (25µm x25 µm), as we aim to produce a retinal implant with 100µm square pixel size stimuli. Our group recently reported that a 3.5°x10° 'window' containing 286 pixels with a 100 µm square size was sufficient to allow reading of 4 letter words at 15° of eccentricity and that a window enlarged to 7°x10° (572 pixels) allowed fluent text reading [38] [39]. Based on these results, we designed stimulating test heads with 4 circular 25 µm radius electrodes and a center-to- center spacing of 150 µm to allow for the generation of pixels >100 µm. The 1000 µm diameter supporting base of our implant head could allow larger electrodes to be fitted if the current small-sized electrodes were unable to provide long term stimulations below the retinal safety threshold**.**

In summary, we have implanted subretinal polyimide electrode platforms in the P23H rat, which provides an appropriate model for adRP in humans. Although the surgical technique is difficult because of the very small globe size, subretinal implants in the P23H rat should provide a valid model for assessing the electrical and

biological modalities of subretinal electrode stimulation with the aim of developing a retinal prosthesis in humans.

FUNDING

The present work was supported by : Swiss National Fund for Scientific Research (grants 3100-61956.00 and 3152-063915.00), Fondation pour les Aveugles (Geneva), Fédération des aveugles et Handicapés Visuels de France, Fondation des Gueules Cassées, INSERM, University Pierre and Marie Curie (Paris VI), Assistance Publique-Hôpitaux de Paris (AP-HP), Fondation Ophtalmologique A. de Rothschild.

ACKNOWLEDGMENTS

The staff of the EPFL Center for MicroNanoTechnology is acknowledged for technical support in the fabrication of the electrodes.

COMPETING INTERESTS: none declared

REFERENCES

1 Stone JL, Barlow WE, Humayun MS *et al*. Morphometric analysis of macular photoreceptors and ganglion cells in retinas with retinitis pigmentosa. *Arch Ophthalmol* 1992;**110**:1634-1639

2 Santos A, Humayun MS, de Juan MS *et al*. Preservation of the inner retina in retinitis pigmentosa. A morphometric analysis. *Arch Ophtalmol* 1997;**115**:511-515

3 Humayun MS, Prince M, de Juan EJ *et al*. Morphometric analysis of the extramacular retina from post-mortem eyes with with retinitis pigmentosa. *Invest Ophthalmol Vis Sci* 1996; **40**:143-148

4 Kim SY, Sadda S, Pearlman J *et al*. Morphometric analysis of the macula in eyes with disciform age-related macular degeneration. *Retina* 2002; **22**:471-7.

5 Kim SY, Sadda S, Humayun MS et al. Morphometric analysis of the macula in eyes with geographic atrophy due to age-related macular degeneration. *Retina* 2002; **22**:464-70.

6 Humayun MS, de Juan E Jr, Dagnelie G et al. Visual perception elicited by electrical stimulation of retina in blind humans. *Arch Ophthalmol* 1996; **114**:40-6.

7 Humayun MS, de Juan E Jr, Weiland JD et al. Pattern electrical stimulation of the human retina. *Vision Res* 1999;**39**:2569-76.

8 Chow AY, Chow VY. Subretinal electrical stimulation of the rabbit retina. *Neurosci Lett* 1997; **225**:13-6.

9 Zrenner E, Miliczek KD, Gabel VP et al. The development of subretinal microphotodiodes for replacement of degenerated photoreceptors. *Ophthalmic Res* 1997;**29**:269-80.

10 Ziegler D, Linderholm P, Mazza M *et al*. An active microphotodiode array of oscillating pixels for retinal stimulation. *Sens Actuators A Phys* 2004;**110**: 11-17

11 Kerdraon YA, Downie JA,Suaning GJ *et al*. Development and surgical implantation of a vision prosthesis model into the ovine eye. *Clin Experiment Ophthalmol* 2002;**30**:36-40

12 Rizzo JF 3rd, Wyatt J, Loewenstein J *et al*. Methods and perceptual thresholds for short-term electrical stimulation of human retina with microelectrode arrays. *Invest Ophthalmol Vis Sci* 2003; **44**:5355-61.

13 Rizzo JF 3rd, Wyatt J, Loewenstein J *et al*. Perceptual efficacy of electrical stimulation of human retina with a microelectrode array during short-term surgical trials. *Invest Ophthalmol Vis Sci* 2003; **44**:5362-9.

14 Eckmiller R. Learning retina implants with epiretinal contacts. *Ophthalmic Res* 1997; **29**:281-9

15 Humayun MS. Intraocular retinal prosthesis. *Trans Am Ophthalmol Soc* 2001;**99**:271-300

16 Humayun MS, Weiland JD, Fujii GY *et al*. Visual perception in a blind subject with a chronic microelectronic retinal prosthesis. *Vision Res* 2003; **43**: 2573-81

17 Veraart C, Raftopoulos C, Mortimer JT et al. Visual sensations produced by optic nerve stimulation using an implanted self-sizing spiral cuff electrode. *Brain Res* 1998; **813**:181-6.

18 Delbeke J, Oozeer M, Veraart C. Position, size and luminosity of phosphenes generated by direct optic nerve stimulation. *Vision Res* 2003; **43**:1091-102.

19 Pardue MT, Stubbs EB Jr, Perlman J *et al*. Immunohistochemical studies of the retina following long-term implantation with subretinal microphotodiode arrays. *Exp Eye Res* 2001; **73**:333-43.

20 Pardue MT, Ball SL, Hetling Jr *et al*. Visual evoked potentials to infrared stimulation in normal cats and rats. *Doc Ophthalmol* 2001; **S103(2)**:155-62.

21 Schanze T, Sachs HG, Wiesenack C et al. Implantation and testing of subretinal film electrodes in domestic pigs. *Exp Eye Res*. 2005 Aug 24; [Epub ahead of print]

22 Sachs HG, Schanze T, Wilms M. Subretinal implantation and testing of polyimide film electrodes in cats. *Graefe's Arch Clin Exp Ophthalmol* 2005; **243**:464-468

23 Pardue MT, Phillips MJ, Yin H *et al*. Neuroprotective effect of subretinal implants in the RCS rat. *Invest Ophthalmol Vis Sci* 2005;**46**:674-82

24 Chow AY, Chow VY, Packo KH *et al*. The artificial silicon retina microchip for the treatment of vision loss from retinitis pigmentosa. *Arch Ophthalmol* 2004;**122**:460-9.

23 Pardue MT, Phillips MJ, Yin H *et al*. Neuroprotective effect of subretinal implants in the RCS rat. *Invest Ophthalmol Vis Sci* 2005; **46**:674-82

25 Metz S, Bertsch A, Bertrand D *et al*. Flexible polyimide probes with microelectrodes and embedded microfluidic channels for simultaneous drug delivery and multi-channel monitoring of bioelectric activity. Biosens Bioelectron 2004;**19**:1309-1318

26 Banisadr G, Queraud-Lesaux F, Boutterin MC *et al*. Distribution, cellular localization and functional role of CCR2 chemokine receptors in adult rat brain. *J Neurochem* 2002;**81**:257-69.

27 Schwahn HN, Gekeler F, Kohler K *et al*. Studies on the feasibility of a subretinal

visual prosthesis: data from Yucatan micropig and rabbit. *Graefes Arch Clin Exp Ophthalmol* 2001;**239**:961-7.

28 Chow AY, Pardue MT, Chow VY *et al*. Implantation of silicon chip microphotodiode arrays into the cat subretinal space. *IEEE Trans Neural Syst Rehabil Eng* 2001;**9**:86-95.

29 Hämmerle H, Kobuch K, Kohler K *et al*. Biostability of microphotodiode arrays for subretinal implantation. *Biomaterials* 2002; 23:797-804

30 Chow AY, Pardue MT, Perlman JI *et al*. Subretinal implantation of semiconductor-based photodiodes: durability of novel implant designs. *J Rehabil Res Dev* 2002; **39**:312-322

31 Zrenner E, Stett A, Weiss S *et al*. Can subretinal microphotodiodes successfully replace degenerated photoreceptors? *Vision Res* 1999;**39**:2555-67.

32 Frasson M, Picaud S, Leveillard T *et al*. Glial cell line-derived neurotrophic factor induces histologic and functional protection of rod photoreceptors in the rd/rd mouse. *Invest Ophthalmol Vis Sci* 1999; **40**:2724-34

33 D'Cruz PM, Yasumura D *et al*. Mutation of the receptor tyrosine kinase gene Mertk in the retinal dystrophic RCS rat. *Hum Mol Genet* 2000;**9**:645-51

34 Machida S, Kondo M, Jamison JA *et al*. P23H rhodopsin transgenic rat: correlation of retinal function with histopathology. *Invest Ophthalmol Vis Sci* 2000;**41**:3200-9

35 Zrenner E. The subretinal implant: can microphotodiode arrays replace degenerated retinal photoreceptors to restore vision? *Ophthalmologica*. 2002;**216**: S1:8-20; discussion 52-3

36 Baig-Silva MS, Hathcock CD, Hetling JR. A preparation for studying electrical stimulation of the retina in vivo in rat. *J Neural Eng* 2005;**2**:S29-38. Epub 2005 Feb 22

37 Grimnes S, Martinsen *0. Bioimpedance and Bioelectricity Basics*, Cornwall, Academic Press 2000:3

38 Sommerhalder J, Oueghlani E, Bagnoud M *et al*. Simulation of artificial vision: I. Eccentric reading of isolated words, and perceptual learning. *Vision Res*. 2003;**43**:269-83.

39 Sommerhalder J, Rappaz B, de Haller R *et al*. Simulation of artificial vision: II. Eccentric reading of full-page text and the learning of this task. *Vision Res* 2004;**44**:1693-706

LEGENDS

Figure 1: Different retinal implant designs which were implanted a) a 3 mm wide device with 4 central stimulating electrodes and a reference elctrode on the 4 sides b) a 1 mm device with four stimulating electrodes and a large circular reference electrode. Some of these were equipped with 25 µm holes for increased diffusion; c) a 250 µm asymmetric implant with only one central electrode.

Figure 2: In vivo SLO images of retinal implants in dystrophic rats. A) Rat fundus showing a 250 µm implant head in the subretinal space. B) Fluorescein angiography obtained 1.5 months after the surgery and showing retinal blood vessels passing above the subretinal 1000 µm implant head

Figure 3: In vivo stimulation for implant impedance measurements. A) Non-anesthetized animal connected to an LCR meter. The Eppendorf cap protecting the external implant connector on the skull is visible. This connector is wired to an LCR meter seen in the background through a switch board (not shown) and four BNC cables. B) Impedance spectra. Impedance measurement obtained at different frequencies with a 50mV sine wave stimulation. The measurements were repeated at the beginning of the experiment (0min, dark 15min (red) and 60 min (blue)).

Figure 4: Retinal semithin section showing the subretinal implant. Note that retinal cells are in apposition to the retinal implant. The scale bar represents 100 µm.

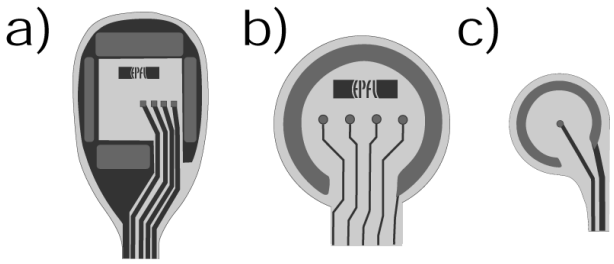

Figure 1

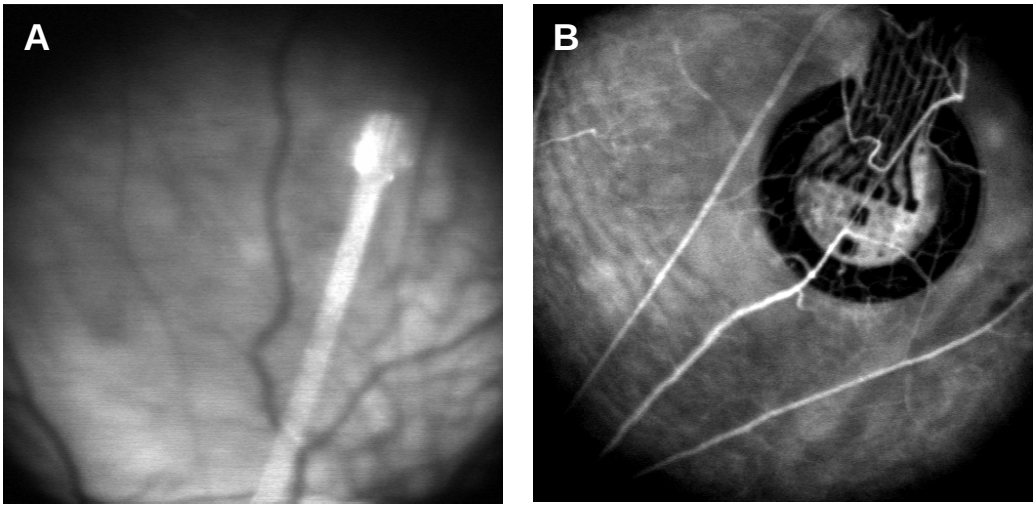

Figure 2

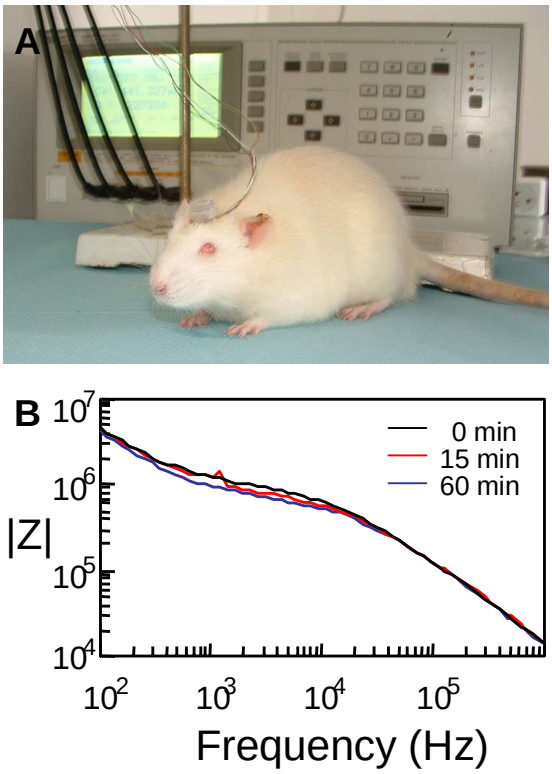
A
B
10^7
10^6
10^5
10^4
|Z|
10^2
10^3
10^4
10^5
Frequency (Hz)
0 min
15 min
60 min

Figure 3

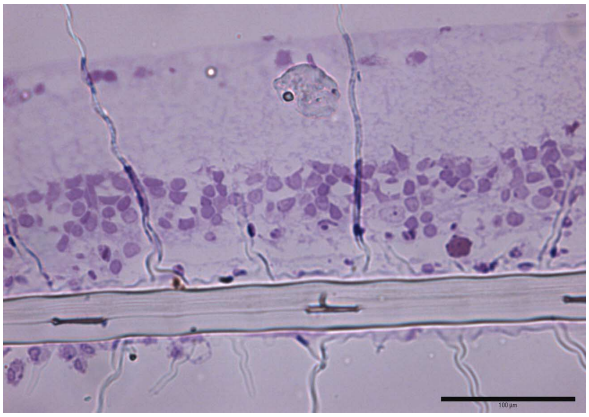

Figure 4